SURFACE AND INTERFACE ANALYSIS
*Surf. Interface Anal.* 2002; **34**: 559–564
Published online in Wiley InterScience (www.interscience.wiley.com). DOI: 10.1002/sia.1419

SIA

# Analysis of the boundaries of $ZrO_2$ and $HfO_2$ thin films by atomic force microscopy and the combined optical method

**Petr Klapetek,[1,2] Ivan Ohlídal,[1]* Daniel Franta[1] and Pavel Pokorný[3]**

[1] Department of Physical Electronics, Faculty of Science, Masaryk University, Kotlářská 2, 611 37 Brno, Czech Republic
[2] Czech Metrology Institute, Okružní 31, 638 00 Brno, Czech Republic
[3] Institute of Scientific Instruments, CAS, Královopolská 147, 612 64 Brno, Czech Republic

Received 28 November 2001; Revised 17 March 2002; Accepted 23 March 2002

**In this paper an atomic force microscopy analysis of the microrough upper boundaries of $ZrO_2$ and $HfO_2$ thin films is presented. Within this analysis the values of the width, root-mean-square value of heights and power spectral density function of these boundaries are determined for $ZrO_2$ and $HfO_2$ exhibiting different thicknesses. The thickness dependences of the quantities mentioned are introduced. The values of the thicknesses of the films are evaluated using the combined optical method. This optical method is also used to describe boundary microroughness within the effective medium theory. A discussion of the results concerning the microroughness of the upper boundaries of both the $ZrO_2$ and $HfO_2$ thin films is also introduced.** **Copyright © 2002 John Wiley & Sons, Ltd.**

**KEYWORDS:** $ZrO_2$ and $HfO_2$ films; rough upper boundaries; AFM; optical methods

## INTRODUCTION

Thin films of $ZrO_2$ (zirconia) and $HfO_2$ (hafnia) are frequently used in practice. In particular these films are employed in the optics industry and therefore attention in the literature has been devoted to studies of their optical properties. In this paper our attention is devoted to the analysis of the structure (roughness) of the upper boundaries of both the zirconia and hafnia films (i.e. the boundaries between the ambient and the films). One can namely expect that this structure can influence the optical properties of these films. For this roughness analysis atomic force microscopy (AFM) is employed. The influence of the thickness values of the films on the upper boundary roughness is studied. The thickness of the films mentioned is determined using the combined optical method based on combining variable angle of incidence spectroscopic ellipsometry and near-normal incidence spectroscopic reflectometry.[1] Moreover, within the effective medium theory (EMT) the boundary roughness of both films is optically characterized as well. A comparison of the AFM and combined optical method results is presented.

## PREPARATION OF SAMPLES AND EXPERIMENTAL ARRANGEMENTS

The $ZrO_2$ films were prepared using vacuum reactive evaporation by an electron gun onto single-crystal silicon wafers. The origin material was ZrO. The substrate temperature was 280 °C and the evaporation rate was $\sim$0.5 nm s$^{-1}$. The vacuum pressure during evaporation was $4 \times 10^{-4}$ mbar. The $HfO_2$ films were prepared using the same technology onto the same substrates. The origin material was $HfO_2$. The substrate temperature was also 280 °C, the evaporation rate was 0.3 nm s$^{-1}$ and the vacuum pressure was $2 \times 10^{-4}$ mbar.

The spectral dependences of the ellipsometric parameters $\psi$ (azimuth) and $\Delta$ (phase change) were measured by a Jobin Yvon UVISEL ellipsometer ($\lambda \in \langle 400, 830\ \text{nm}\rangle$ and $\theta_0 \in \langle 55, 75^\circ\rangle$, where $\lambda$ and $\theta_0$ are the wavelength and the angle of incidence, respectively). The spectral dependences of the reflectance $R$ were measured using a Varian Cary 5E spectrophotometer within the same spectral region ($\theta_0 = 10^\circ$). The AFM measurements were performed using a commercial Accurex Topometrix atomic force microscope.

The upper boundaries of the zirconia and hafnia films were measured using AFM in the following way: scanned area from $1 \times 1$ up to $2.5 \times 2.5$ μm, tube scanner (max range $2.5 \times 2.5 \times 0.8$ μm), scan rate $<2$ μm s$^{-1}$, standard non-contact tip (apex ratio 1:5, apex curvature $<10$ nm) and sharpened contact tip (apex ratio 1:10, apex curvature $<20$ nm).

## DATA PROCESSING

### Processing of the AFM data

It is known that some artifacts (systematic errors) can appear in the AFM measurements of fine structures. The main artifact is the 'tip convolution' caused by the tip finite sharpness. This effect misrepresents the measurement of the

*Correspondence to: Ivan Ohlídal, Department of Physical Electronics, Faculty of Science, Masaryk University, Kotlářská 2, 611 37 Brno, Czech Republic. E-mail: ohlidal@physics.muni.cz
Contract/grant sponsor: Grant Agency of Czech Republic;
Contract/grant numbers: 101/01/1104; 202/01/1110.

Copyright © 2002 John Wiley & Sons, Ltd.

microroughness of a film. In particular, the lateral dimensions of all measured objects, including the roughness, are enlarged in AFM images. This fact affects the values of the parameters characterizing the boundary roughness investigated. It is therefore necessary to correct this artifact in a suitable way. In the literature there are several procedures for this correction (see Refs 2–4). We have used the procedure of Villarubia,[3] called 'surface reconstruction'.

Note that before applying Villarubia's procedure the AFM data must be corrected for the low-frequency noise in the slow scan direction. Villarubia's procedure is based on using the rough surface as its own tip characterizer and the procedure has been employed because the geometry of the tip changed slightly during the measurements so it was not possible to use the other modification of Villarubia's procedure by using a separate tip characterizer.

After reconstructing the measured boundaries we carried out the statistical analysis of the microroughness data. First we determined the boundary width $W(L)$, defined as (see Ref. 5)

$$W^2(L) = \left\langle [h(x, y) - \langle h(x, y)\rangle]^2 \right\rangle \tag{1}$$

where $h(x, y)$ represents the boundary heights, $x$ and $y$ denote the Cartesian coordinates in the mean plane of the boundary and the angled brackets denote statistical averaging over the area $L^2$. It is known that[5]

$$W(L) \begin{cases} \sim L^{\alpha}, & (L < L_c) \\ = \sigma, & (L > L_c) \end{cases} \tag{2}$$

where $\alpha$ is the roughness exponent related to the fractal dimension of the rough boundaries studied and $\sigma$ denotes the root-mean-square (RMS) value of the height in the conventional meaning corresponding to a sufficiently large scale (i.e. for lengths $L$ larger than a certain critical length $L_c$).

Further, we determined the values of the power spectral density function (PSDF) of the microrough upper boundaries of the zirconia and hafnia thin films. This function is defined as[6,7]

$$W_1(K_x) = \frac{2\pi}{LM} \sum_{j=0}^{M} |H_j(K_x)|^2 \tag{3}$$

where $H(K_x)$ is a one-dimensional Fourier transform given as follows

$$H_j(K_x) = \frac{\Delta}{2\pi} \sum_m h_j(m\Delta) \exp[-i(K_x m\Delta)] \tag{4}$$

where $\Delta$ is the distance between adjacent points of the recorded AFM scan, $M$ denotes the number of the rows within the scan and $K_x$ denotes the component of the wave vector of the harmonic component corresponding to a certain spatial frequency of roughness.

It should be noted that the values of $H_j(K_x)$ are calculated using the fast Fourier transform.

### Processing of the optical data

For treating the optical data the least-squares method (LSM) is employed. The merit function is identical to that used in our foregoing paper,[1] i.e.

$$S(\vec{X}) = \sum_i |\hat{\rho}(\vec{X}) - \hat{\rho}_i|^2 w_i + \sum_j [R(\vec{X}) - R_j]^2 w_j \tag{5}$$

where vector $\vec{X}$ has components identical to the parameters sought, complex quantity $\hat{\rho}$ is expressed as $\hat{\rho} = \hat{r}_p/\hat{r}_s = \tan(\psi)\exp(i\Delta)$, $r_p$ and $r_s$ denote the reflection Fresnel coefficient of the system for $p$- and/or $s$-polarization, respectively, and $\psi$ and $\Delta$ are the azimuth and phase change, respectively. Symbols $i$ and $j$ correspond to the summation over experimental values of $\hat{\rho}_i$ and $R_j$, respectively, and $w_i$ and $w_j$ denote the weight of the individual experimental values. The LSM used is based on the Marquardt-Levenberg algorithm.[8]

The ellipsometric parameters and reflectance of the films are calculated using the formulae derived by means of the matrix formalism (see Refs 9–11). It is assumed that the zirconia and hafnia films exhibit the inhomogeneity formed by a profile in refractive index across the films. This inhomogeneity was found in our earlier optical studies of these films (see Refs 1 and 12). The function representing the refractive index profiles of the inhomogeneous $ZrO_2$ and $HfO_2$ thin films is parameterized as follows

$$n^2(z, \lambda) = n_R^2(\lambda)p(z) + n_L^2(\lambda)[1 - p(z)] \tag{6}$$

where $n_L(\lambda)$ and $n_R(\lambda)$ are the refractive indices of the upper and lower boundaries of the inhomogeneous film, respectively, and the function $p(z)$ is expressed as[12]

$$p(z) = Ae^{-az/d} + Be^{-b(1-z/d)} + c \tag{7}$$

where

$$A = -\frac{c + (1-c)e^{-b}}{1 - e^{-a-b}}, \qquad B = \frac{1 - c + ce^{-a}}{1 - e^{-a-b}} \tag{8}$$

In the foregoing equations the symbol $d$ denotes the thickness of the inhomogeneous film and $a$, $b$ and $c$ are parameters. Function $n_L(\lambda)$ is fixed at unity (it is assumed that the ambient is formed by air) and function $n_R(\lambda)$ is expressed using the Cauchy formula, i.e. $n_R = A_R + B_R/\lambda^2$. The optical model of both of the films studied is plotted schematically in Fig. 1. The values of the constants $A_R$ and $B_R$ are fixed at values corresponding to the refractive indices of the bulk materials $ZrO_2$ and $HfO_2$ (see Ref. 13). This means that the zirconia and hafnia films are characterized by four optical parameters, i.e. by parameters $a$, $b$, $c$ and $d$. The values of these parameters were determined by treatment of the experimental data using the LSM [see Eqn. (5)]. In Table 1 the values of the parameters $a$, $b$, $c$ and $d$ determined in this way are summarized for all the samples of $HfO_2$ and $ZrO_2$ studied.

## RESULTS

In Fig. 2 a typical AFM image of the upper boundary of one $HfO_2$ film is presented. Similar AFM images were obtained for the other hafnia and zirconia thin films. In Fig. 3 the refractive index profile $n(z)$ adjacent to the ambient for this $HfO_2$ film is plotted for $\lambda = 600$ nm. It is evident that part of this refractive index profile can be used to describe the microroughness of this boundary. This statement is implied by the EMT. Within the EMT the microrough boundary is represented by a transition layer whose refractive index varies continuously between the two values corresponding

Copyright © 2002 John Wiley & Sons, Ltd.

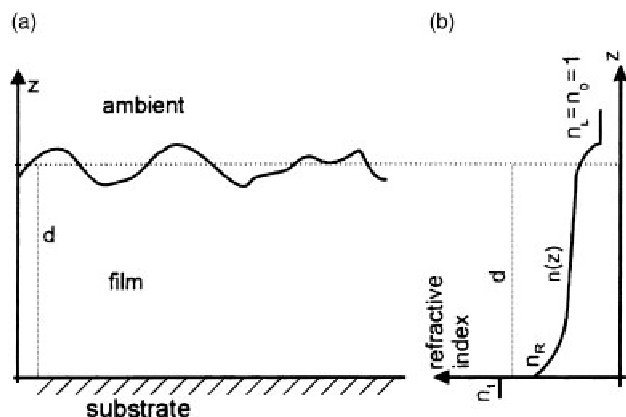


**Figure 1.** (a) Schematic diagram of the geometrical model of the films under investigation. (b) Schematic diagram of the corresponding optical model of these films. Symbols $d, n_1, n(z), n_0, n_L$ and $n_R$ denote the thickness of the film, the refractive indices of the substrate, film and ambient and the refractive index value adjacent to the ambient and substrate, respectively. Symbol $z$ represents the coordinate of the $z$-axis perpendicular to the boundary between the substrate and film.

**Table 1.** The values of $a$, $b$, $c$ and $d$ for the $ZrO_2$ and $HfO_2$ thin films studied[a]

| Sample | $d$ (nm) | $a$ | $b$ | $c$ |
|---|---|---|---|---|
| A1 | $1007 \pm 1$ | $73.59 \pm 0.15$ | $30.48 \pm 0.06$ | $0.760 \pm 0.001$ |
| A2 | $502.8 \pm 0.4$ | $56.69 \pm 0.69$ | $25.51 \pm 0.42$ | $0.750 \pm 0.001$ |
| A3 | $745.3 \pm 0.8$ | $61.80 \pm 0.16$ | $32.79 \pm 0.11$ | $0.758 \pm 0.001$ |
| A4 | $290.9 \pm 0.2$ | $38.55 \pm 0.36$ | $14.93 \pm 0.19$ | $0.760 \pm 0.001$ |
| B1 | $648.2 \pm 0.4$ | $127.6 \pm 1.10$ | $21.04 \pm 0.22$ | $0.872 \pm 0.001$ |
| B2 | $336.7 \pm 0.2$ | $70.79 \pm 0.76$ | $5.69 \pm 0.18$ | $0.876 \pm 0.001$ |
| B3 | $183.82 \pm 0.05$ | $59.11 \pm 0.28$ | $2.57 \pm 0.03$ | $0.866 \pm 0.001$ |
| B4 | $61.73 \pm 0.03$ | $45.07 \pm 2.30$ | $5.45 \pm 1.03$ | $0.934 \pm 0.003$ |

[a] Symbols A1–A4 and B1–B4 represent the samples of the zirconia and hafnia films, respectively (see text).

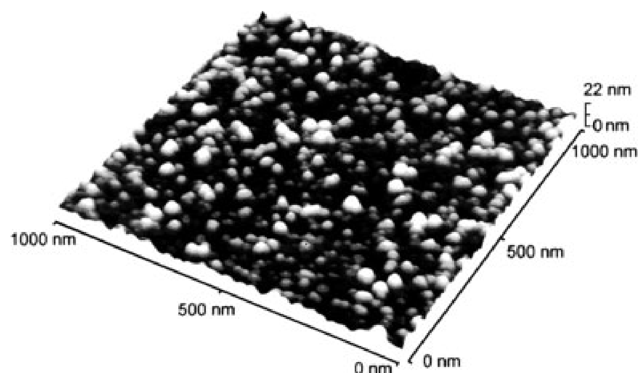


**Figure 2.** The AFM picture of the part of the upper boundary of the chosen hafnia film (sample B3).

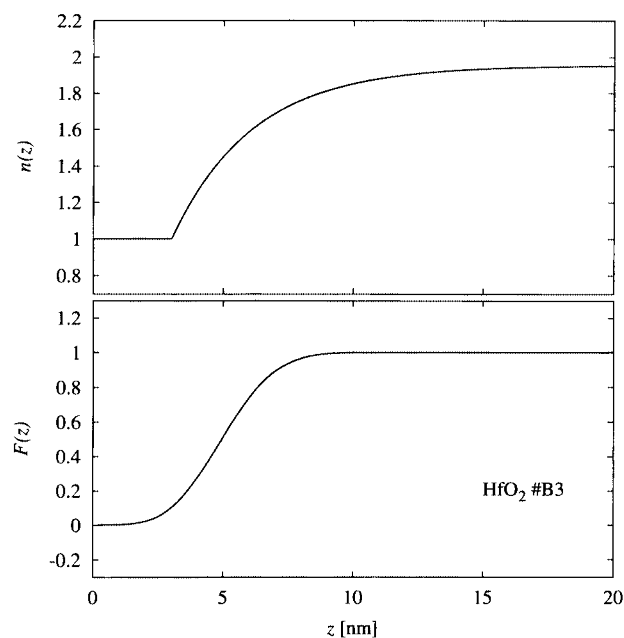


**Figure 3.** The profile of the refractive index $n(z)$ of the chosen hafnia film (sample B3) adjacent to the upper boundary, determined by the optical method, and the cumulative distribution function of the heights of the upper boundary $F(z)$ of the same film evaluated by AFM ($z$ denotes the coordinate corresponding to the axis perpendicular to the boundaries). Note that the graph of the profile of the refractive index $n(z)$ is shifted along the $z$-axis for clarity (profile $n(z)$ starts from the value $n(z) = 1$, i.e. the value $n(z) = 1$ must set in $z = 0$ only).

to the media adjacent to this boundary (see Refs 9 and 14). Note that the EMT can be used to describe the microrough boundaries if the linear dimensions of their roughness are substantially smaller than the wavelength of light incident onto these boundaries, which is fulfilled for the boundaries of both the zirconia and hafnia films studied here (see Fig. 2). From Eqns (6)–(8) and Fig. 3 one can see that the value of the parameter $d/a$ equals a length proportional to the RMS value of the microroughness of the upper boundaries from the optical point of view. The value of $d/a$ determines the form of the profile of the refractive index $n(z)$ of the film adjacent to the upper boundary of the film. By increasing the value of $d/a$ the width of the profile of $n(z)$ increases in this region, and vice versa. Moreover, the gradient of $n(z)$ within the region mentioned decreases with increasing $d/a$, and vice versa. The RMS value $\sigma$ has the same influences on the behaviour of the cumulative distribution function $F(z)$ of the heights of the upper boundary. It is known that this function $F(z)$ coincides with the profile of the refractive index $n(z)$ of the fictitious thin film representing the surface roughness within the EMT (for details see Ref. 15). Thus, one can deduce that the quantity $d/a$ is proportional to the RMS value $\sigma$. In Fig. 3 the cumulative distribution function $F(z)$ of the heights of the upper boundary of this hafnia film determined using AFM is plotted. Similar refractive index profiles and AFM height distribution functions were found for the other hafnia and zirconia films.

In Table 2 the values of thicknesses $d$, $\sigma$ and $d/a$ of all the zirconia (A1–A4) and hafnia (B1–B4) films studied are summarized. The dependences of $\sigma$ and $d/a$ on thickness presented in Table 2 are plotted in Fig. 4. Note that the values of $d/a$ were determined under the assumption that the

Copyright © 2002 John Wiley & Sons, Ltd.

**Table 2.** The values of $\sigma$ and $d/a$ for the different thicknesses of both the zirconia and hafnia thin films

| Sample | $d$ (nm) | $\sigma$ (nm) | $d/a$ (nm) |
|---|---|---|---|
| A1 | $1007 \pm 1$ | $6.9 \pm 0.2$ | $13.68 \pm 0.05$ |
| A2 | $502.8 \pm 0.4$ | $3.8 \pm 0.1$ | $8.88 \pm 0.11$ |
| A3 | $745.3 \pm 0.8$ | $4.3 \pm 0.2$ | $12.06 \pm 0.05$ |
| A4 | $290.9 \pm 0.2$ | $2.0 \pm 0.1$ | $7.55 \pm 0.08$ |
| B1 | $648.2 \pm 0.4$ | $3.4 \pm 0.2$ | $5.10 \pm 0.04$ |
| B2 | $336.7 \pm 0.2$ | $4.2 \pm 0.2$ | $4.76 \pm 0.06$ |
| B3 | $183.82 \pm 0.05$ | $3.2 \pm 0.1$ | $3.11 \pm 0.02$ |
| B4 | $61.73 \pm 0.03$ | $0.77 \pm 0.08$ | $1.37 \pm 0.06$ |

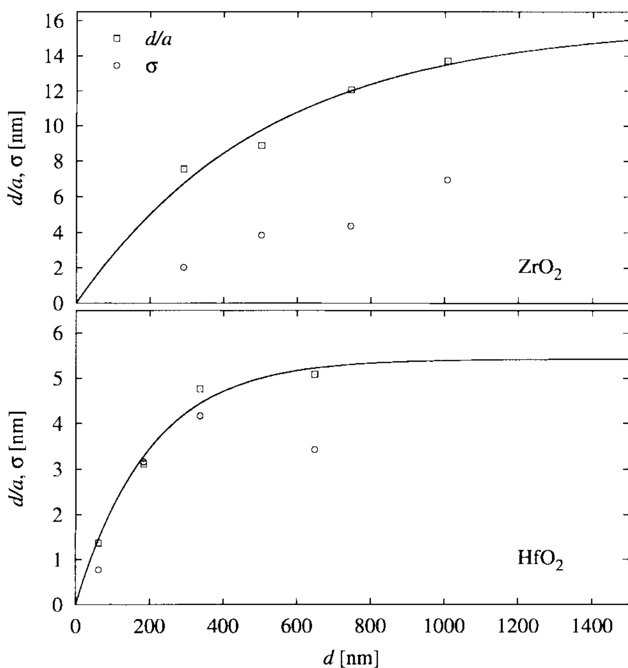


**Figure 4.** The thickness dependences of $\sigma$ and $d/a$ for the zirconia and hafnia films studied: the points denote the experimental values of $\sigma$ and $d/a$; the curves correspond to the function $d/a = A[1 - \exp(-d/B)]$.

thickness dependence of this quantity is

$$d/a = C[1 - \exp(-d/D)] \quad (9)$$

The parameters found are: $C = 5.4 \pm 0.3$ nm and $D = 198 \pm 35$ nm for the hafnia films; and $C = 15 \pm 2$ nm and $D = 520 \pm 150$ nm for the zirconia films. The foregoing values of $C$ and $D$ have been determined by fitting the values of $d/a$ introduced in Fig. 4 and Table 2 by means of the function presented in Eqn. (9) using the LSM.

The other relevant dependences describing the properties of the boundaries of interest, i.e. the dependences of the width $W(L)$ on the scale $L$ and the PSDF on $K_x$, are plotted in Figs 5 and 6, respectively. From Fig. 5 it can be estimated that the threshold values of $L$ (i.e. the value of $L_c$) for the hafnia and/or zirconia films are ~200 and 500 nm, respectively. Moreover, from the dependences presented in Fig. 5 one can determine the roughness exponent $\alpha$ of the boundaries studied [see Eqn. (2)]. We found that the values of $\alpha$ lie within the interval 0.4–0.7 for both films.

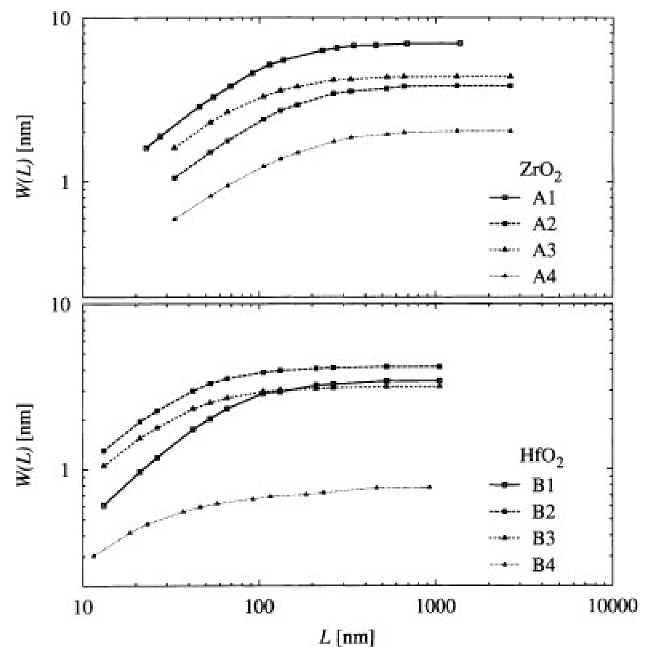


**Figure 5.** The dependences of the boundary width on the length of the side $L$ of the area used for its evaluation.

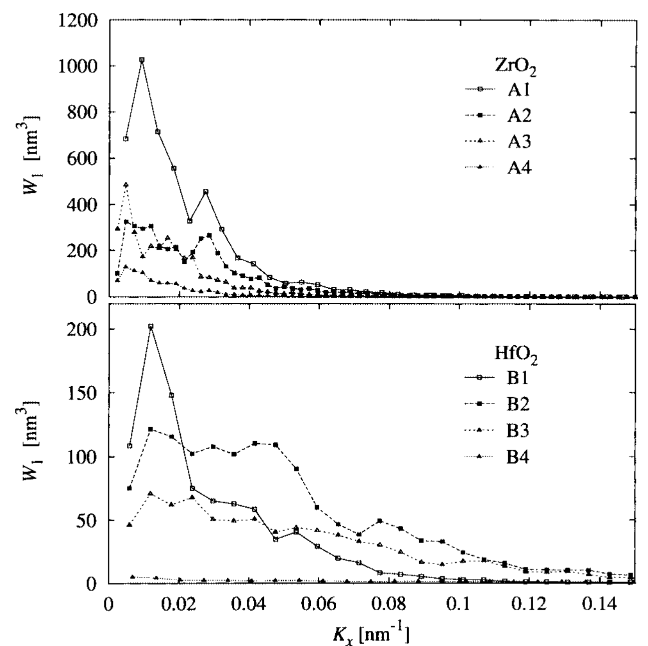


**Figure 6.** The PSDF of the upper boundaries of the zirconia and hafnia films.

## DISCUSSION

It is known that the zirconia and hafnia films exhibit the columnar structure (see Refs 16–18). Films with a columnar structure have rough upper boundaries (see Refs 19 and 20) and thus the measured microroughness represents the form and dimensions of the tops of the columns in the films.

The function $F(z)$ in Fig. 3 supports the fact that within the EMT the transition layer representing the microrough boundaries must exhibit a continuous profile of the refractive index. Moreover, one can see that the course of $F(z)$ coincides with the form of the refractive index profile adjacent to

Copyright © 2002 John Wiley & Sons, Ltd.

the ambient to be plotted in the same figure. Thus, this course of $F(z)$ shows that the part of the refractive index profile $n(z)$ plotted in Fig. 3 represents the roughness of the upper boundary of the hafnia film in a reasonable way. From both Table 2 and Fig. 4 it is clear that the values of $\sigma$ and $d/a$ are mutually different (this statement is true for the $ZrO_2$ films in particular). This is caused by the fact that the quantities $\sigma$ and $d/a$ are not strictly identical (i.e. they are defined mathematically in different ways). Nevertheless, these parameters have been compared because both refer to the heights of the surface roughness. The zirconia films are rougher than hafnia films. Moreover, $d/a$ converges to a constant value corresponding to the value of parameter $C$ that is different for both materials. The same property can be expected for the dependences of $\sigma$ on the values of thickness (see Fig. 4).

From Fig. 5 it is seen that the values of $\sigma$ determined by AFM must be evaluated for sufficiently large areas of the boundary (i.e. for sufficiently large values of $L$). This fact is important from the practical point of view because it implies that before calculating the values of $\sigma$ one has to estimate the value of $L_c$ for every columnar thin film under study. If the area employed for measuring is not sufficiently large, a strong misrepresentation of the results for the quantities mentioned above can be obtained.

From the dependences of the PSDF (see Fig. 6) one can see that the hafnia boundaries comprise the roughness components characterized with higher spatial frequencies than the zirconia boundaries. From this fact it is possible to imply that the boundary roughness of the $HfO_2$ films is finer compared with the boundary roughness of the $ZrO_2$ films. This conclusion further implies that the $HfO_2$ columnar structure is finer than that of $ZrO_2$, i.e. the columns and pores are narrower for the hafnia films than for zirconia films. Note that the curves $W_1(K_x)$ of the individual zirconia and hafnia films coincide with the values of $\sigma$ determined for these films (see Table 2 and Fig. 6). This statement is implied by the validity of the following equation

$$\sigma^2 = \int_{-\infty}^{\infty} W_1(K_x)\mathrm{d}K_x \qquad (10)$$

The areas under the curves representing $W_1(K_x)$ thus equal the values of $\sigma$ for the individual samples.

Of course, the pores between the columns influence the microroughness of the upper boundaries as well, but the influence of the pores on the measured microroughness also depends on the penetration of the tip into the pores. There is a procedure for evaluating the areas of the surface of boundary that the tip, with a given geometry, cannot touch at a single point (see Ref. 3). In this case there is an impossibility in determining the profile of the boundary in the vicinity of such points. Thus, the profile of the microrough boundary can be misrepresented here. The situation arises when the tip can penetrate a pore only partially. Using the chosen tip, it is then possible to record an 'effective' microroughness of the upper boundaries related to the columnar structure of the films investigated. It is also evident that the values of the quantities characterizing the 'effective' boundary microroughness of

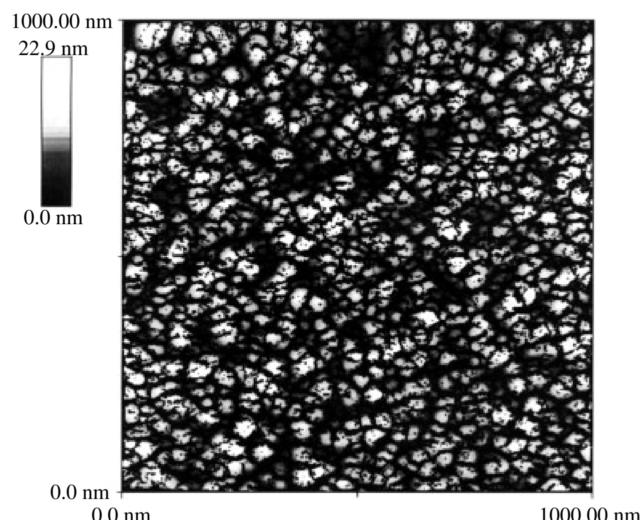


**Figure 7.** The certainty map of the part of the upper boundary of the chosen hafnia film (sample B3). The black areas denote the areas at which the the tip cannot touch the material of the film at a single point (for details, see Ref. 3).

the columnar films are dependent on the geometry of the tip used.

Using the procedure mentioned above, the areas corresponding to the impossibility of touching the tip with the surface at single points for the chosen hafnia film are plotted in Fig. 7 (black areas) together with the surface topography of this film. Note that in some places the black areas coincide with the tops of the columns. This fact is caused by noise remaining in the picture, in spite of noise correction.

## CONCLUSION

In this paper the results of AFM and optical studies of the microroughness of the upper boundaries of the zirconia and hafnia films are presented. It was shown that AFM in combining with the optical methods was usable for studying the roughness of the films because the main quantities describing this roughness could be determined using this technique. The values of the quantities characterizing the microroughness heights and the power spectral density function of the films with different thicknesses were determined. It was shown that the heights of the surface roughness of the upper boundaries of both the hafnia and zirconia films increased as the thickness of these films increased. The zirconia films were rougher than hafnia ones. The microroughness of the hafnia films contained the roughness components with the higher spatial frequencies than the zirconia films, which implied that the columnar structure of the hafnia films was finer than the structure of the zirconia films. This fact is apparently caused by the difference in the mobilities of the particles of $ZrO_2$ and $HfO_2$ on the surfaces of the substrates in the initial stages of forming these films.

### Acknowledgements
The authors wish to thank the researchers of the Supercomputing Centre of the Masaryk University, Brno, for their help with the

Copyright © 2002 John Wiley & Sons, Ltd.

numerical computations. Further, the authors are indebted to Dr K. Navrátil for performing the reflectance measurements.

This work was supported by the Grant Agency of Czech Republic under contracts 101/01/1104 and 202/01/1110.

## REFERENCES

1. Franta D, Ohlídal I. *Surf. Interface Anal.* 2000; **30**: 574.
2. Markiewicz P, Goh MC. *J. Vac. Sci. Technol. B* 1995; **13**: 1115.
3. Villarubia JS. *J. Res. Natl. Inst. Stand. Technol.* 1997; **102**: 425.
4. Nagy P, Márk GI, Balázs E. *Mikrochim. Acta Suppl.* 1996; **13**: 425.
5. Yoshinobu T, Iwamoto A, Sudoh K, Iwasaki H. *J. Vac. Sci. Technol. B* 1995; **13**: 1630.
6. Dumas P, Bouffakhredine B, Amra C, Vatel O, Andre E, Galindo R, Salvan F. *Europhys. Lett.* 1993; **22**: 717.
7. Franta D, Ohlídal I, Klapetek P. *Mikrochim. Acta* 2000; **132**: 443.
8. Marquardt WD. *J. Soc. Ind. Appl. Math.* 1963; **11**: 431.
9. Ohlídal I, Franta D. *Progress in Optics*, vol. 41, Wolf E (ed.). Elsevier: Amsterdam, 2000; 181–282.
10. Ohlídal I, Franta D, Pinčík E, Ohlídal M. *Surf. Interface Anal.* 1999; **28**: 240.
11. Ohlídal I, Franta D. *Acta Phys. Slov.* 2000; **50**: 489.
12. Franta D, Ohlídal I, Klapetek P, Pokorný P, Ohlídal M. *Surf. Interface Anal.* 2001; **32**: 91.
13. Aleksandrov VI, Kalabukhova VF, Lemonova EE, Osiko VV, Tatarintsev VI. *Inorg. Mater.* 1977; **13**: 1747.
14. Aspnes DE, Theeten JB, Hottier F. *Phys. Rev. B* 1979; **20**: 288.
15. Nèvot L, Croce P. *Rev. Phys. Appl.* 1980; **15**: 761.
16. Cho HJ, Hwangbo Ch K. *Appl. Opt.* 1996; **35**: 5545.
17. Ben Amor S, Rogier B, Baud G, Jacquet M, Nardin M. *Mater. Sci. Eng.* 1998; **B57**: 28.
18. Zuber A, Jänchen H, Kaiser N. *Appl. Opt.* 1996; **35**: 5553.
19. Ritter E. *Appl. Opt.* 1976; **15**: 2318.
20. Pulker HK. *Appl. Opt.* 1979; **18**: 1969.

Copyright © 2002 John Wiley & Sons, Ltd.